

The low-energy ARPES and heat capacity of $\text{Na}_{0.3}\text{CoO}_2$: A DMFT study

C. A. Marianetti¹, K. Haule^{1, 2}, and O. Parcollet²

¹*Department of Physics and Astronomy and Center for Condensed Matter Theory,
Rutgers University, Piscataway, NJ 08854-8019 and*

²*Service de Physique Theorique, CEA/DSM/SPHT-CNRS/SPM/URA 2306 CEA/Saclay, F-91191 Gif-Sur-Yvette, France*

(Dated: December 19, 2018)

We use the dynamical mean-field theory (DMFT) to calculate the angle resolved photoemission spectrum (ARPES) and heat capacity for $\text{Na}_{0.3}\text{CoO}_2$. Both the traditional Hirsch-Fye Quantum Monte-Carlo technique and the newly developed continuous time quantum Monte-Carlo technique are used to solve the DMFT impurity problem. We show that the e'_g hole pockets on the Fermi surface are suppressed as the on-site coulomb repulsion is increased. A quantitative comparison with ARPES experiments and bulk heat capacity measurements indicate that the on-site coulomb repulsion is large relative to the LDA bandwidth.

The cobaltates have demonstrated a wide variety complex behavior. The Na rich region of the phase diagram displays various degrees of anomalous behavior, such as Curie-Weiss behavior near a band insulator[1], charge disproportionation[2], and non-Fermi-liquid behavior in the resistivity[1]. Alternatively, the Na poor region of the phase diagram appears to be a Fermi-liquid. The magnetic susceptibility displays Pauli behavior, the resistivity is roughly quadratic at low temperatures[1], and the system appears to be homogeneous[2]. Therefore, the Na poor region of the phase diagram seems like a natural starting point to attempt to explain the ARPES experiments and heat capacity measurements from a quantitative standpoint.

In Na_xCoO_2 , the cubic component of the oxygen crystal field splits the Co d manifold into a set of 3-fold t_{2g} orbitals and 2-fold e_g orbitals, while the trigonal component will further split the t_{2g} orbitals into a_{1g} and e'_g . The nominal valence of Co in this system will be $4-x$, so the Fermi-energy will fall within the t_{2g} manifold. The LDA band structure displays two degenerate eigenvalues and one non-degenerate eigenvalue at the Γ -point, corresponding to the e'_g and a_{1g} eigenvectors. The splitting between the eigenvalues is roughly 1 eV with the e'_g levels below the Fermi energy and the a_{1g} above. Despite this distinct splitting at the Γ -point, the on-site orbital energies are nearly degenerate. Additionally, the projected density-of-states (DOS) clearly show that the a_{1g} orbital character is strongest at the top and bottom of the band while the e'_g is present through most of the energy range of the t_{2g} bands. The Fermi surface consists of a large a_{1g} pocket around the Γ -point and six small e'_g satellite pockets[3].

Several experimental ARPES studies have been performed for $\text{Na}_{0.3}\text{CoO}_2$ [4, 5, 6, 7]. A general caricature of the LDA bands can be seen in the ARPES. The most notable difference as compared to LDA is the significant narrowing of the bands, and the suppression of the e'_g pockets below the Fermi energy. Two previous studies addressed the effect of correlations on the electronic structure for $x = 0.3$, and they reached completely oppo-

site conclusions. Zhou et al performed Gutzwiller calculations for a three-band model corresponding to the LDA t_{2g} band structure[8]. Using an infinite on-site coulomb repulsion, they show that the quasi-particle bands are significantly narrowed and the e'_g hole pockets are pushed beneath the Fermi surface. Although the removal of the e'_g pockets agrees with the ARPES experiments, it is not clear if $U = \infty$ is an excessive assumption and therefore smaller values of the on-site coulomb repulsion must be considered. Ishida et al[9] performed DMFT calculations for the three-band t_{2g} states of the cobaltates and found that electronic correlations narrow the bands and enhance the e'_g hole pockets, completely opposite to what was found by Zhou et al.

Singh et al. have proposed that the inclusion of the realistic ordering of the Na destroys the e'_g hole pockets, as demonstrated by LDA calculations for $\text{Na}_{0.7}\text{CoO}_2$ [10]. Given that the pockets will inevitably be destroyed as $x \rightarrow 1$ because the chemical potential moves towards the top of the t_{2g} bands, $\text{Na}_{0.7}\text{CoO}_2$ is an extremely liberal test case in which the pockets are barely present in the first place. Previous LDA calculations of the realistic structure which explicitly included the Na, both with and without water, had already shown that LDA predicts the survival of the pockets for $\text{Na}_{\frac{1}{3}}\text{CoO}_2$ [11, 12], even when including full structural relaxations [11]. Therefore, one can safely conclude that the Na potential is not the dominant mechanism which destroys the pockets in $\text{Na}_{0.3}\text{CoO}_2$.

In this study, we resolve the issue of the qualitative behavior of the pockets. We calculate the ARPES spectrum and the heat capacity at a range of different U in order to determine the best agreement with experiment. In particular, we focus on the presence or absence of the pockets, the linear coefficient of the heat capacity, and the average Fermi velocity measured in ARPES. The presence or absence of the pockets will have important consequences for the heat capacity given that they are the dominant contribution to the DOS at the Fermi energy, and therefore these two issues are intimately connected.

We perform DMFT calculations for the t_{2g} bands of the

cobaltates, represented by the following Hamiltonian:

$$H = \sum_{ij\alpha\beta\sigma} t_{\alpha\beta} c_{i\alpha\sigma}^\dagger c_{j\beta\sigma} + \sum_{i\alpha\beta\sigma\sigma'} U_{\alpha\beta}^{\sigma\sigma'} n_{i\alpha\sigma} n_{i\beta\sigma'} + \sum_{i\sigma} \Delta (n_{a_{1g}i\sigma} - n_{e'_g i\sigma}) \quad (1)$$

where α, β are the orbital indices (ie. a_{1g} and e'_g), i, j are site indices, σ is the spin index, and Δ is the crystal-field splitting between the a_{1g} and e'_g orbitals. We use the low-energy hopping parameters $t_{\alpha\beta}$ and Δ which were fit to the LDA t_{2g} bands by Zhou et al[8], allowing for a direct comparison. Ishida et al did not publish their hopping parameters, but they appear to be similar given the respective bare DOS which were published[9]. We assume the traditional orbital-independent double counting[13] of $U(N - \frac{1}{2})$, and therefore the Hartree-Fock terms generated by DMFT will be relevant. Below we will show that Δ is a key parameter in determining the fate of the e'_g pockets and therefore the heat capacity. Given that LDA is only an approximate technique to generate the low energy hopping parameters, we will systematically explore the effect of Δ on the results. The LDA value fit by Zhou et al is roughly $\Delta = -10\text{meV}$, and therefore the on-site orbital energies are nearly degenerate. Alternatively, quantum chemistry calculations[14] yield a value of 300meV , so one might anticipate $-10\text{meV} \leq \Delta \leq 300\text{meV}$.

DMFT maps the interacting lattice problem onto an impurity problem where the non-interacting bath function is determined self-consistently [15]. The effective impurity problem is solved using two different impurity solvers to ensure that the answer is robust. The traditional Hirsch-Fye quantum Monte-Carlo (HFQMC) method was used (see ref [13, 15] for detailed review), in addition to the newly developed continuous time quantum Monte-Carlo (CTQMC) method [16, 17]. CTQMC is generally more efficient than the HFQMC and allows one to access significantly lower temperatures and larger U .

The e'_g pockets are observed in the k-space direction corresponding to the real-space direction which connects nearest-neighbor Co atoms. ARPES experiments predict the e'_g pockets to be below the Fermi energy[4, 5, 6, 7], and this is supported by the analysis of the de Haas van Alphen experiments [18]. Given that two previous theoretical studies reach opposite conclusions regarding the fate of the e'_g pockets, we explore this question in detail. When determining the Fermi surface from the Dyson equation, only the bare Hamiltonian and the self-energy at zero frequency are needed [19]. Within single-site DMFT the self-energy is momentum-independent and therefore the self-energy at zero frequency acts as a renormalization of the on-site e'_g and a_{1g} energy levels. Therefore, it is useful to reverse-engineer this problem and determine what effective e'_g and a_{1g} levels are

needed to destroy the pockets. This is not a-priori obvious given that the neighboring e'_g - a_{1g} hopping is comparable to the a_{1g} - a_{1g} hopping. We find that the pockets are completely insensitive to perturbations of the a_{1g} on-site energy. The pockets are destroyed when the e'_g on-site energy is shifted down by roughly 70meV , independent of the value of the perturbation of the a_{1g} level, and therefore the criterion for the destruction of the pockets is $\Sigma_{e'_g} - \mu < -70\text{meV}$. This is an important observation which indicates that a relatively small perturbation of the e_g on-site energy will destroy the pockets. DMFT calculations can now be performed to determine when this criterion is satisfied.

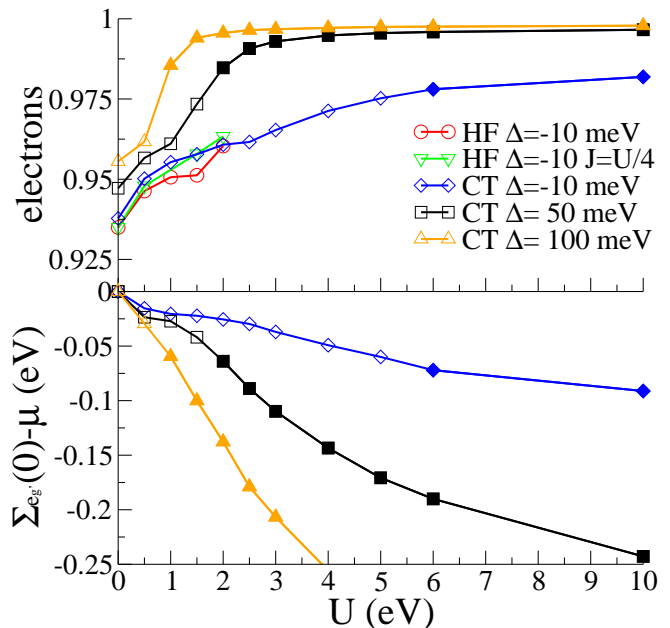


FIG. 1: a.) e'_g orbital occupation as a function of U . The a_{1g} orbital occupation can be found from the relation $n_{a_{1g}} = 5.3 - 2n_{e'_g}$. HFQMC and CTQMC calculations were performed at $\beta = 40\text{eV}^{-1}$ and $\beta = 100\text{eV}^{-1}$, respectively. Filled points indicate that the pockets have been destroyed. b.) The self-energy of the e'_g orbital at zero frequency minus the chemical potential for various values of the crystal field splitting Δ ($\Delta = -10\text{meV}$ corresponds to the LDA crystal field).

$\Sigma_{e'_g} - \mu$ is found to be a monotonically decreasing function of U , which indicates that the pockets are *diminished* with increasing interactions (see figure 1 b). The quantity $\Sigma_{a_{1g}} - \mu$ is a monotonically increasing function of U (not pictured). Considering the dynamical portion of the self-energy (ie. $\Sigma_{dyn}(i\omega) = \Sigma(i\omega) - \Sigma(\infty)$), we find that $\Sigma_{dyn}^{e'_g}(0) > \Sigma_{dyn}^{a_{1g}}(0)$, but this is countered by the fact that $\Sigma^{a_{1g}}(\infty) > \Sigma^{e'_g}(\infty)$ and the net result is that $\Sigma^{a_{1g}}(0) > \Sigma^{e'_g}(0)$. Therefore, the destruction of the pockets is due entirely to the static Hartree contribution to the self-energy (ie. $\Sigma(\infty)$). The dynamical contribution of the self-energy actually enhances the pockets,

but ultimately the static part of the self-energy dominates and the net effect is that increasing interactions diminishes the pockets. The preceding analysis is true for both the CTQMC and the HFQMC impurity solvers. The two solvers agree completely on a qualitative level, and are quantitatively similar for small U while more significant differences arise for larger U due to discretization errors within the HF method. We also plot the orbital occupations as a function of U (see figure 1a), which indicates an enhancement of orbital polarization as U is increased, consistent with the destruction of the pockets. This conclusion is found for both the CTQMC and HFQMC solvers, and this holds even when an on-site exchange coupling (ie. $-Jn_{\alpha\sigma}n_{\beta\sigma}$) is included in the HFQMC method. Exchange had little effect on the results, in agreement with Ishida et al [9].

Having established the qualitative behavior of the pockets, we continue with more quantitative analysis. Given that only a 70 meV downward shift of the e_g on-site energy is required to destroy the pockets, we believe that it is useful to probe the behavior of the self-energy for other values of Δ as rationalized above. The CTQMC calculations were repeated for $\Delta = 50\text{meV}$ and $\Delta = 100\text{meV}$. As anticipated, starting with a crystal field splitting which diminishes the pockets acts cooperatively with interactions and causes the system to polarize more and the pockets to be destroyed for a smaller U (see figure 1 a and b). For $\Delta = 50\text{meV}$ the pockets are destroyed for $U \geq 2.0\text{eV}$, while for $\Delta = 100\text{meV}$ the pockets are destroyed for $U \geq 1.0\text{eV}$. Therefore, we conclude that the value of U required to destroy the pockets depends strongly on the value of Δ .

Our findings are in qualitative agreement with Zhou et al[8] and in qualitative disagreement with Ishida et al[9]. It is not clear why the results of Ishida et al are different, but it is likely the result of differences in the bare Hamiltonian. Above we showed that the static correlations diminish the pockets while the dynamic correlations enhance the pockets, and the balance of these two effects will be influenced by the bare Hamiltonian. Regardless, our following analysis of the Fermi velocity and heat capacity will demonstrate that the destruction of the pockets is the only viable possibility to achieve agreement with experiment.

Having understood the behavior of the pockets, we now compute the linear coefficient of the heat capacity, γ . We use Fermi-liquid theory to calculate γ from the DOS at the Fermi energy and the quasiparticle weight Z which is calculated in our QMC calculations. Mathematically, we have $\gamma = \frac{2\pi k_B^2}{3} \sum_{\alpha} \frac{\rho_{\alpha}(0)}{Z_{\alpha}}$, where α corresponds to the orbital index and ρ is the local spectral function[13]. The experimentally measured heat capacities for $\text{Na}_{0.3}\text{CoO}_2$ are found to be in the range of $12\text{-}16 \frac{\text{mJ}}{\text{mol-Co-K}^2}$ [20, 21, 22, 23, 24, 25]. We begin by noting that the heat capacity is $14.27 \frac{\text{mJ}}{\text{mol-Co-K}^2}$ for the LDA

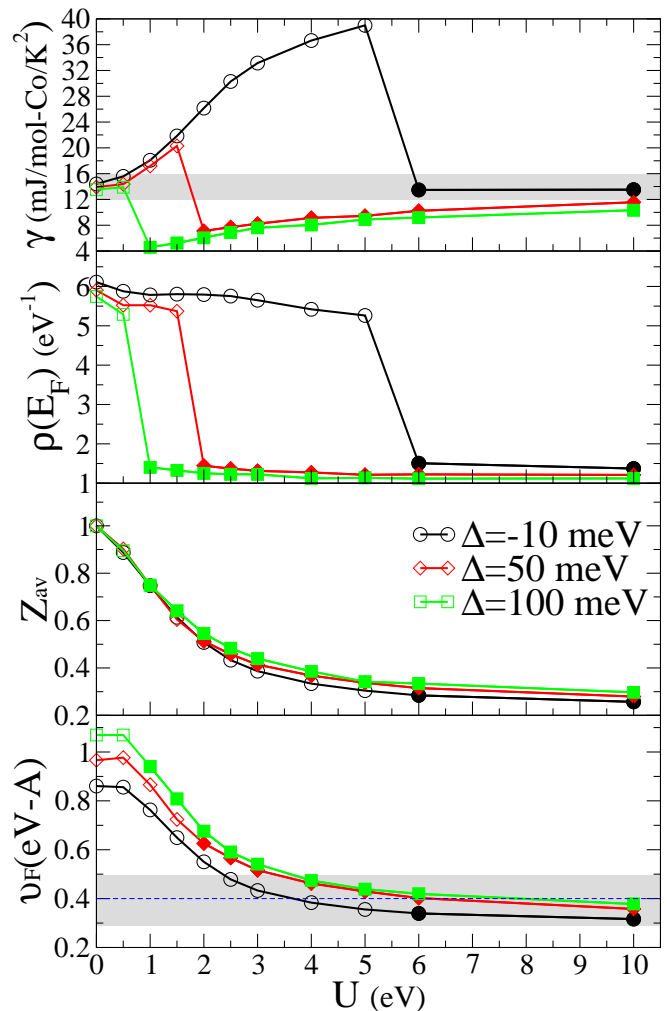


FIG. 2: The heat capacity, density-of-states at the Fermi energy, the quasiparticle weight Z , and the average of the absolute value of the Fermi velocity for the Γ -M and Γ -K directions are shown in panels a, b, c, and d, respectively. Filled points indicate that the pockets have been destroyed. The shaded region in panel a corresponds to the range of experimentally measured values of γ . The blue dotted line in panel d corresponds to the experimentally measured Fermi velocity, while the grey shading corresponds to the error bar [5].

hoppings, which is already within the bounds of experimental measurements. This may mislead one to believe that correlations are negligible, but a more careful examination shows otherwise. The DOS at the Fermi energy initially decreases weakly as U increases and eventually drops in a discontinuous fashion, which signifies the destruction of the pockets (see figure 2). The quasiparticle weight also decreases as U increases. Given that the linear coefficient of the heat capacity is proportional to the ratio $\frac{\rho(e_f)}{Z}$, the overall effect is not a priori obvious. The heat capacity initially increases as U increases, then discontinuously drops when the pockets are destroyed, and

eventually plateaus for large U . Increasing Δ causes the drop in the heat capacity to occur at smaller values of U and a overall lower value for the heat capacity. In order to achieve agreement with experimental measurements of the heat capacity, one needs a relatively large $U = 6eV$ when using the LDA Δ , and even larger U is needed for larger Δ . A key point is that if the pockets are retained, the γ becomes excessively large as U increases. Given that the ARPES indicates that the bandwidth is nearly halved as compared to LDA, an appreciable U must be present to narrow the LDA bands and if the pockets were still present the heat capacity would be excessive as compared to experiment. It is reasonable to expect that the heat capacity should be under-predicted when only considering the Hubbard model. There will likely be electron-phonon coupling to the local breathing mode of the octahedron, or perhaps other modes, which will induce a narrowing of the bands and therefore an enhancement of the heat capacity.

The experimentally measured Fermi velocity may also be calculated as a function of U (see figure 2). Increasing the U decreases the quasiparticle weight Z and therefore decreases the Fermi velocity. In order to achieve velocities comparable with experiment, one needs a relatively large $U > 3eV$. This is another piece of evidence, independent of the heat capacity measurements, which indicates that the U must be relatively large. Once again, if the U is large then the pockets must be absent in order to get acceptable agreement with the heat capacity.

Both impurity solvers used in this study work on the imaginary axis, and therefore one must perform an analytic continuation to access real frequency quantities like the ARPES spectrum. Various approaches exist to perform the analytic continuation, but all are approximate. We expand the self-energy to first-order, which allows an exact analytic continuation, and use the resulting self-energy to construct the low energy ARPES spectrum (see figure 3). The first case corresponds to the $\Delta = -10meV$ and $U = 6eV$, the minimum to destroy the pockets for this case (see figure 3a). As shown, the pockets are too close to the Fermi energy, and the bands are excessively narrow as compared to experiment. Increasing to $U = 10eV$ will further sink the pockets, but it will also continue to narrow the bandwidth. Alternatively, one may decrease the U slightly if the Δ is increased as the pockets are suppressed at a much lower U . Therefore, we examine the ARPES for $\Delta = 50meV$ and $U = 4eV$, and $\Delta = 100meV$ and $U = 4eV$ (see figure 3b and 3c). Decreasing U and increasing Δ increases the bandwidth and pulls the pockets down further, putting the result in better agreement with experiment. This analysis suggests that optimum U should be chosen from the lower end of the range of values deduced from the analysis of the heat capacity and the velocity, and that Δ should be slightly larger than the one deduced from LDA.

In conclusion, we have examined the issue of the e'_g

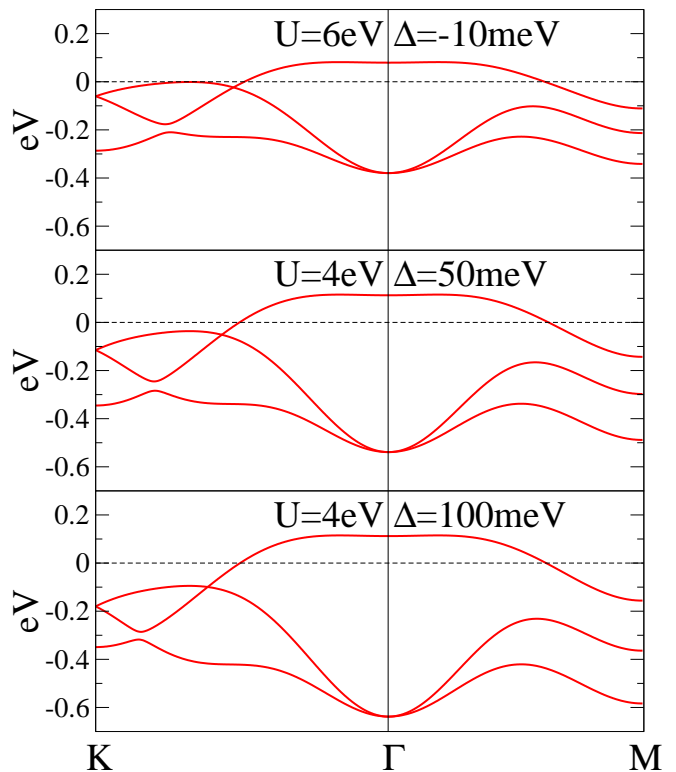


FIG. 3: The ARPES for a.) $U = 6.0$ $\Delta = -10meV$ b.) $U = 4.0$ $\Delta = 50meV$ c.) $U = 4.0$ $\Delta = 100meV$. All calculations performed at $\beta = 100eV^{-1}$.

pockets, the value of the linear coefficient of the heat capacity, and the Fermi velocity. We have demonstrated that increasing interactions destabilize the e'_g pockets and pushes them beneath the Fermi energy. This is in agreement with previous calculations of Zhou et al[8] and in disagreement with previous calculations of Ishida et al[9]. Reasonable agreement can be achieved with both bulk heat capacity measurements and the Fermi velocity measured by ARPES when using an on-site coulomb repulsion which is several times the LDA bandwidth (ie. $U > 4eV$).

We acknowledge useful discussions with G. Kotliar, P.A. Lee, H. Ding, and M.Z. Hasan. Funding was provided by NSF under grant DMR 0528969. C.A. Marianetti acknowledges funding from ICAM.

-
- [1] M. L. Foo, Y. Y. Wang, S. Watauchi, H. W. Zandbergen, T. He, R. J. Cava, and N. P. Ong, Phys. Rev. Lett. **92**, 247001 (2004).
 - [2] I. R. Mukhamedshin, H. Alloul, G. Collin, and N. Blanchard, Phys. Rev. Lett. **94**, 247602 (2005).
 - [3] D. J. Singh, Phys. Rev. B **61**, 13397 (2000).
 - [4] H. B. Yang, Z. H. Pan, A. K. P. Sekharan, T. Sato, S. Souma, T. Takahashi, R. Jin, B. C. Sales, D. Mandrus, A. V. Fedorov, et al., Phys. Rev. Lett. **95**, 146401

- (2005).
- [5] D. Qian, L. Wray, D. Hsieh, D. Wu, J. L. Luo, N. L. Wang, A. Kuprin, A. Fedorov, R. J. Cava, L. Viciu, et al., *Phys. Rev. Lett.* **96**, 046407 (2006).
- [6] D. Qian, L. Wray, D. Hsieh, L. Viciu, R. J. Cava, J. L. Luo, D. Wu, N. L. Wang, and M. Z. Hasan, *Phys. Rev. Lett.* **97**, 186405 (2006).
- [7] D. Qian, D. Hsieh, L. Wray, Y. D. Chuang, A. Fedorov, D. Wu, J. L. Luo, L. Wang, L. Viciu, R. J. Cava, et al., *Phys. Rev. Lett.* **96**, 216405 (2006).
- [8] S. Zhou, M. Gao, H. Ding, P. A. Lee, and Z. Q. Wang, *Phys. Rev. Lett.* **94**, 206401 (2005).
- [9] H. Ishida, M. D. Johannes, and A. Liebsch, *Phys. Rev. Lett.* **94**, 196401 (2005).
- [10] D. J. Singh and D. Kasinathan, *Phys. Rev. Lett.* **97**, 016404 (2006).
- [11] C. A. Marianetti, G. Kotliar, and G. Ceder, *Phys. Rev. Lett.* **92**, 196405 (2004).
- [12] M. D. Johannes and D. J. Singh, *Phys. Rev. B* **70**, 014507 (2004).
- [13] G. Kotliar, S. Y. Savrasov, K. Haule, V. S. Oudovenko, O. Parcollet, and C. A. Marianetti, *Rev. Mod. Phys.* **78**, 865 (2006).
- [14] S. Landron and M. B. Lepetit, *Phys. Rev. B* **74**, 184507 (2006).
- [15] A. Georges, G. Kotliar, W. Krauth, and M. J. Rozenberg, *Rev. Mod. Phys.* **68**, 13 (1996).
- [16] P. Werner and A. J. Millis, *Cond-mat/0607136* (2006).
- [17] K. Haule, *Cond-mat/0612172* (2006).
- [18] L. Balicas, J. G. Analytis, Y. J. Jo, K. Storr, H. Zandbergen, Y. Xin, N. E. Hussey, F. C. Chou, and P. A. Lee, *Phys. Rev. Lett.* **97**, 126401 (2006).
- [19] F. Lechermann, S. Biermann, and A. Georges, *Prog. Theor. Phys. Sup. p.* 233 (2005).
- [20] G. H. Cao, C. M. Feng, Y. Xu, W. Lu, J. Q. Shen, M. H. Fang, and Z. A. Xu, *Journal Of Physics-condensed Matter* **15**, L519 (2003).
- [21] B. G. Ueland, P. Schiffer, R. E. Schaak, M. L. Foo, V. L. Miller, and R. J. Cava, *Physica C-superconductivity And Its Applications* **402**, 27 (2004).
- [22] F. C. Chou, J. H. Cho, P. A. Lee, E. T. Abel, K. Matan, and Y. S. Lee, *Phys. Rev. Lett.* **92**, 157004 (2004).
- [23] B. Lorenz, J. Cmaidalka, R. L. Meng, and C. W. Chu, *Physica C-superconductivity And Its Applications* **402**, 106 (2004).
- [24] R. Jin, B. C. Sales, S. Li, and D. Mandrus, *Phys. Rev. B* **72**, 060512 (2005).
- [25] N. Oeschler, R. A. Fisher, N. E. Phillips, J. E. Gordon, M. L. Foo, and R. J. Cava, *Physica B-condensed Matter* **359**, 479 (2005).